Estimation of the Hydraulic Conductivity Function of Unsaturated Clays Using Infiltration Column Tests

McCartney, J.S.
The University of Texas at Austin, Texas, USA, jmccartney@mail.utexas.edu

Villar, L. F. S.
Universidade Federal de Minas Gerais, Brazil, lvillar@etg.ufmg.br

Zornberg, J.G.
The University of Texas at Austin, Texas, USA, zornberg@mail.utexas.edu

Abstract: An infiltration column test was performed on a clay specimen with the goal of obtaining the hydraulic conductivity function (K-function). The test was conducted by applying a steady moisture flux to the upper surface of a 750 mm-thick clay profile compacted within a 200-mm diameter column. Transient moisture content variations with height in the soil profile during infiltration were measured using time domain reflectometry (TDR). Steady-state moisture profiles and the transient instantaneous profile method were used to define the K-function. Calculation of the K-function from the transient infiltration data was found to be particularly sensitive to fluctuations in the moisture content time series, so sigmoid curves were fitted to the data. Data was used for the transient analysis until the wetting front reached the base of the soils profile, as the outflow boundary had a significant effect on the moisture profile. The experimentally-defined K-function did not match well with those predicted from the shape of the water retention curve.

Keywords: K-function; Instantaneous Profile Method; Infiltration.

1 INTRODUCTION

1.1 The Hydraulic Conductivity Function

In geotechnical analyses, the hydraulic conductivity of a rigid, water-saturated soil is typically considered to be constant with changes in pore water pressure, assuming steady flow, constant temperature, and no changes in water or soil chemistry. However, this assumption cannot be made for the hydraulic conductivity with changes in negative pore water pressure (referred to as the suction ψ when the air pressure is atmospheric), as the soil becomes unsaturated (*i.e.*, air and water are present in the voids). The relationship between hydraulic conductivity and volumetric moisture content θ, also referred to as the K-function, represents the change in the proportionality between the flow rate and gradient in an unsaturated soil. As the moisture content of a soil decreases, the total number of pathways along which fluid can travel decreases. Accordingly, the K-function is a measure of the increased impedance to moisture flow with decreasing moisture content.

K-functions for geotechnical materials predicted are shown in Figure 1. The hydraulic conductivity values measured for different soils vary over several orders of magnitude, from 1×10^{-14} to 1×10^{-4} m/s. At high volumetric moisture content values, coarser-grained soils have high hydraulic conductivity, while finer-grained soils have lower hydraulic conductivity. The rate of decrease in hydraulic conductivity of coarse-grained soils with decreasing moisture content is steeper than that of fine-grained soils.
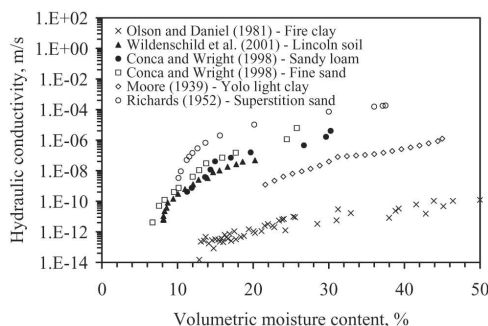
Figure 1. Experimental K-functions for different soils.

1.2 Prediction of the K-function

Early approaches to predict the K-function were empirical. For example, Gardner (1958) proposed an exponential model:

$$K = K_s e^{-\alpha\psi} \tag{1}$$

where K_s is the hydraulic conductivity of a saturated soil, and a is a fitting parameter. The volumetric moisture content can be substituted with the suction using the water retention curve (WRC). Although this model is particularly useful for analytical solution of the governing equation for fluid flow in unsaturated soils (Richards' equation), it does not provide a good fit to the experimental data in Figure 1. Statistical models based on pore size distributions were used later, with the goal of predicting the K-function from the water retention curve (Childs and Collis-George 1950; Burdine 1953; Mualem 1976). These approaches assume that the soil is an interconnected series of pores having a size distribution characterized by the shape of the WRC. The models have the form:

$$\frac{K(\theta)}{K_s} = \left(\frac{\theta - \theta_r}{\theta_s - \theta_r}\right)^b \left(\frac{\int_0^\Theta \frac{dx}{\psi^{2-r}(x)}}{\int_0^1 \frac{dx}{\psi^{2-r}(x)}}\right)^m \tag{2}$$

where b, r, and m are constants related to the pore size distribution, and x is an integration variable. The first term in Equation (6) is a correction factor used to account for tortuosity, while the second term is a ratio between the available (water filled) flow pathways and the total possible number of flow pathways. Burdine (1953) suggested that $b = 2$, $r = 0$, and $m = 1$, while Mualem (1976) suggested that $b = 0.5$, $r = 1$, and $m = 2$. Mualem's assumption is considered to be more suitable for fine-grained soils. The K-function can be predicted from the WRC by inserting a θ-ψ relationship into Equation (2). A commonly used predictive K-function is obtained by substituting the van Genuchten (1980) WRC model into the Mualem form of Equation (2), although there are other models. Statistical models neglect physicochemical effects (attraction of water to particles) on moisture flow and neglect flow of water in films on particle surfaces. Film transport is relevant for flow at low moisture contents (Conca and Wright 1990).

1.3 Laboratory Measurement of the K-function

Several techniques have been proposed for direct determination of the K-function in the laboratory (Benson and Gribb 1997). The simplest approach involves surface evaporation from a soil specimen placed on a laboratory scale. The approach may require significant time good control of the temperature and humidity in the laboratory (Wendroth et al. 1993). The K-function can also be defined using the outflow data from pressure plate or hanging column approaches (Gardner 1956). These approaches require careful measurement of outflow, must account for the impedance to flow due to the ceramic, and should consider the impact of air diffusion through the ceramic on the measurements of outflow volume. The most commonly used technique is the multi-step outflow method, which involves the application of pressure increments selected to ensure a measurable amount of water outflow (Parker et al. 1985; Wildenschild et al. 2001). Several assumptions have been used to infer the K-function from the outflow results, including analytical techniques (Gardner 1956) and inverse solutions (Eching and Hopmans 1993; van Dam et al. 1994). There are other variations of this method that involve either smooth increases in air pressure or a single abrupt pressure increment, but the results of these methods are difficult to interpret and may cause soil volume changes (Butters and Duchateau 2002).

A simple alternative that has been used extensively to alleviate the testing problems listed above is the measurement of the K-function during moisture flow through a specimen confined within a column or permeameter (Moore 1939; Richards 1952). Flow is applied to one end of the soil using either a system of saturated ceramics or a flow pump. Moisture content and suction time series are measured with distance through he soils during infiltration. The data can either be analyzed from the transient infiltration data, or from the steady-state moisture profiles.

During steady vertical infiltration with a deep water table, a unit hydraulic gradient (i.e., $i = 1$) is typically observed in the soil profile, which means that the suction does not change with depth and water flow is driven only by gravity. In this case, the hydraulic conductivity equals the imposed steady-state discharge velocity. Points on the K-function can be obtained by changing the imposed flow. Steady state approaches typically yield repeatable results, but require significant testing times. This is especially the case for dense soils and clays, and for measurement of low hydraulic conductivity values.

The K-function can also be characterized during transient infiltration or evaporation. Transient approaches yield a significant amount of data in a short amount of time, but the results are prone to experimental and calculation errors (Benson and Gribb 1999). Transient infiltration may also be influenced by fingering or preferential flow channels, depending on the soil type.

1.4 Instantaneous Profile Method

An approach to define the K-function from transient infiltration data is the instantaneous profile method (Watson 1966; Hamilton *et al.* 1981; Meerdink *et al.* 1996). This method is a discretization of Darcy's law for vertical flow:

$$K_i = \frac{\Delta V_i}{A \Delta t} \left(\frac{-1}{\left(dh/dz \right)_i} \right) \qquad (3)$$

where z is the height from the specimen base, $\Delta V_{w,i}$ is the volume of water that has passed a point i in the soil profile during an time interval Δt, A is the cross-sectional area of the specimen, and h is the total hydraulic head, equal to:

$$h = z + \frac{u_w}{\gamma_w} \qquad (4)$$

where γ_w is the unit weight of water, and u_w is the (negative) water pressure in the soil, with units of kPa. It is assumed that the osmotic potential of the soil does not vary with water content, so it is not included in Equation (4). Assuming the air pressure in the unsaturated soil is zero, the suction, equal to $(u_a - u_w)$, may be substituted for the water pressure, as follows:

$$h = z - \frac{\psi}{\gamma_w} \qquad (5)$$

The gradient term in Equation (3) can be calculated at each point as follows:

$$i_i = -1 - \frac{1}{\gamma_w} \left(\frac{\psi_i - \psi_{i-1}}{z_{i-1} - z_i} \right) \qquad (6)$$

where $i = 0$ at the upper soil surface, which is at a constant suction value during infiltration. For vertical downward infiltration, the position i increases with depth from the surface. The gradient is typically large during transient infiltration into a compacted soil (*i.e.*, with an initial suction typically greater than 150 kPa).

The suction values in Equation (6) can be measured using tensiometers or heat dissipation units. However, this approach may lead to significant errors in the calculation of the K-function. For instance, there may be timing issues related to the measurement of suction using tensiometers. Water must flow into or out of the tensiometer as the suction in the soil changes, resulting in a time delay that may not correspond to TDR measurements of ΔV_w. Further,

heat dissipation units may not provide adequate resolution at low suction values (< 20 kPa) that occur during infiltration. This was the case during the infiltration test performed for this study. However, heat dissipation units provide an excellent alternative if evaporation were used instead of infiltration.

Alternatively, the gradient can be inferred from moisture content data measured using TDR by calculating the suction values from the WRC. Hysteresis in the WRC may result in some uncertainty. Specifically, infiltration occurs along a hysteresis scanning curve in the WRC, so this approach is only an approximation. In this case, the transient WRC can be defined using simultaneous tensiometer and TDR measurements of suction and moisture content. The drying WRC was used in this study as it fits the transient WRC at high suctions, when HDU suction measurements were reliable.

During a given time interval Δt and depth interval z_i, the volume of water downstream from a given point can be obtained by integrating the water content profile, as follows;

$$\Delta V_{w,i}^j = A \sum_{i=1}^{n} \left(\theta^j - \theta^{j-1} \right) \left(z_{i+1} - z_i \right) \qquad (7)$$

where j represents the current time step, and n is the total number of points.

2 MATERIALS AND METHODS

2.1 Soil Characteristics

The low plasticity clay (CL) used in this study has a specific gravity of 2.71, an average plasticity index of 12, and an average liquid limit of 27. For the infiltration test described in this study, the clay was placed at a target relative compaction (RC) of 70% with respect to the maximum dry density obtained from the standard Proctor test (1902 kg/m^3) at 1% dry of the optimum moisture content of 11.7%. The compaction energy was controlled using a piston compactor with a 40-mm diameter rod and a pressure of 10 psi. The hydraulic conductivity of the saturated clay was 6.6x10^{-6} m/s, obtained using a flexible-wall permeameter. The specimen was back-pressure saturated with tap water as the permeating fluid. An effective stress of 7 kPa was used, along with a hydraulic gradient of 2.0. The hanging column and pressure plate methods (Wang and Benson 2004) were used to define drying-path WRCs for the clay soil. The WRC results shown in Figure 2 indicate that the clay has a porosity of 49.2%, an air entry value of 1 kPa and a residual moisture content of approximately 5%.
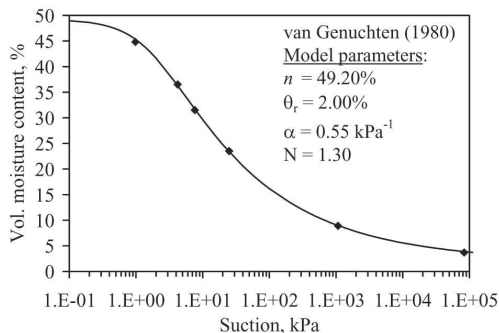
Figure 2. Water characteristic curve (WRC) for the CL clay placed at a relative compaction of 70%.

2.2 Moisture Monitoring Equipment

During infiltration, volumetric moisture content values at different points in the soil column were inferred using time domain reflectometry (TDR). TDR involves interpretation of the reflected waveform for an electromagnetic pulse applied to a transmission line terminating in a shielded, metallic, waveguide (Topp *et al.* 1980). The waveguide is buried within the soil mass. The pulse is reflected at every change in impedance along the transmission line-probe system (*e.g.*, the beginning and end of the waveguide). The travel time of the reflected pulse in the waveguide is related to the dielectric permittivity of the soil mass as follows:

$$K_a = \left(\frac{c\Delta t}{2L}\right)^2 \tag{8}$$

where c is the speed of light, and *l* is the length of the waveguide. As the dielectric permittivity of water is an order of magnitude greater than that of air and soil particles, the dielectric permittivity calculated from the travel time correlates well with the volumetric moisture content. For the CL clay placed at 70% relative compaction, the calibration curve was:

$$\theta = 14.9\sqrt{K_a} - 23.4 \tag{9}$$

Suction was also measured in this study using heat dissipation units. However, these sensors show poor sensitivity for low suctions (< 20 kPa) present during infiltration, so they are not discussed.

2.3 Experimental Setup

A PVC column permeameter shown in Figure 3 having an inside diameter of 203 mm was used for testing. The large diameter was selected to minimize leakage along the side wall of the permeameter, and to provide a large area of water flow. A soil profile thickness of

0.75 m was selected to minimize boundary effects on the moisture content profile during infiltration.
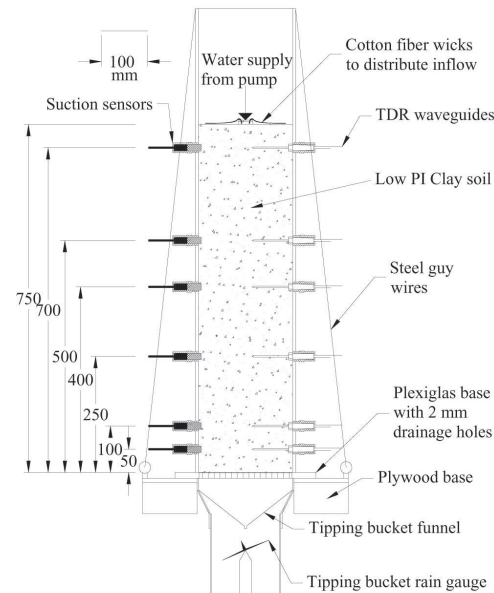
Figure 3. Schematic of soil column.

The large size of the columns required several custom-built components to provide hydraulic sealing and a sturdy working environment during preparation of the soil profile. The PVC columns were attached to the frame using tensioned wires. The wires were attached to eye bolts affixed to a plywood support, and hook bolts were placed over the top edge of the column. A turnbuckle was used to tension the wire, placing the wire in tension. The base of the column rests on an acrylic plate with a 195-mm diameter honey-comb pattern of 2 mm holes. This acrylic plate was intended to serve as a freely-draining lower boundary to the soil column. The column was sealed to the acrylic plate using an o-ring placed within a groove in the base of the column. Outflow was measured using a tipping-bucket rain gauge.

A constant water flow rate was applied to the top surface of the soil using a Masterflex® L/S peristaltic pump. The pump functions by compressing a nylon tube against a series of 6.35 mm rolling barrels on a circular frame. The circular frame is rotated about its center by a motor at a constant rate. Small packets of water are trapped in the tube between each rolling barrel, providing a pulsing flow rate. The connection between the tubing and the pump is frictional, so the tubing was refreshed every 3 weeks to prevent changes in the flow rate due wear. The height of water in a 1000 ml graduated cylinder was monitored as a backup.

Due to the low flow rates used in this study, the distribution of the fluid over the area of the column was challenging. The inflow line from the peristaltic pump was placed within a small cup at the center of the soil area, and the fluid was distributed across the top of the of the soil surface using a radial assembly of fabric wicks. Moisture content measurements at different locations across the soil surface indicate that the water distribution is relatively uniform.

2.4 Procedures

Before placement of soil within the column, a thin film of vacuum grease was placed on the inside wall of the column. This was intended to help minimize side-wall leakage during infiltration and minimize friction during compaction. Moisture conditioned soil was then compacted in 25 mm lifts using the piston compactor. The actual relative compaction was 72.4%. TDR waveguides were installed within the middle of lifts during compaction. A rubber stopper with a central hole was used to provide a seal between the TDR wiring and the column. The heights of the TDR waveguides for the different profiles are shown in Figure 3. The waveguides were initially placed in the loose lift with a slight upward orientation so that they would be horizontal after compaction. Post-test examination indicated that this was the case.

3   RESULTS

3.1 Inflow-Outflow Data

The inflow and outflow volumes of water for the soil profile are shown in Figure 4(a). Two inflow stages were used in this study. The first inflow stage involved application of a constant inflow rate of 8×10^{-8} m/s until steady-state seepage was observed, which required about 1500 hrs. The second inflow stage involved application of a higher rate of 1.5×10^{-7} m/s, and continued until steady seepage was observed, after about 2000 hrs. The progression of the wetting front during infiltration is shown in Figure 4(b). This figure indicates that approximately 550 hrs were required for the wetting front to reach the base of the profile. However, the tipping bucket data in Figure 4(b) indicates that outflow did not occur until 950 hrs. This occurs due to boundary effects on the moisture profile. Water did not exit from the soil until the base of the profile was nearly saturated, which was caused due to the capillary break effect. A capillary break forms when there is a contrast in pore sizes at an interface, (i.e., the fine-grained CL clay placed atop the relatively large holes in the outflow platen).

(a)

(b)
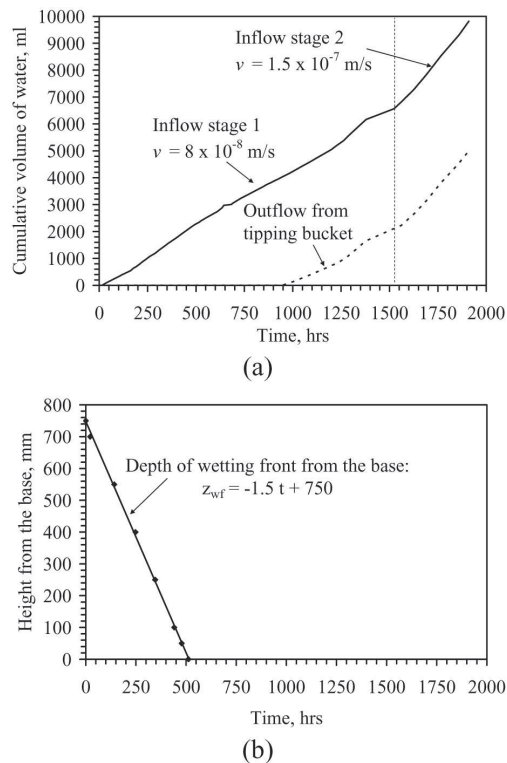
Figure 4. (a) Inflow and outflow data; (b) Wetting front progression.

3.2 Moisture Content Time Series

The moisture content time series inferred from the six TDR waveguides are shown in Figure 5. At the beginning of testing, the moisture content in the column is uniformly equal to 14.7% (corresponding to the molding gravimetric water content of 10.7%). As the wetting front passes through the profile, the moisture content measured by TDR increases gradually to approximately 23.5%. After the wetting front reaches the base at a time of 520 hrs (see Figure 4), the TDR measurements indicate that moisture begins to accumulate in the lower portion of the profile. The moisture content begins to progressively increase with height in the column up to a height of 500 mm. By the time outflow is collected from the base of the column, the moisture content at a height of 50 mm from the base is 40% (degree of saturation of 0.81). The final gravimetric moisture content at the base after testing was 47% (nearly saturated). During accumulation of moisture at the base of the profile, the upper portion of the profile was relatively unaffected by the boundary, and is only influenced by on-going infiltration. For instance, when the

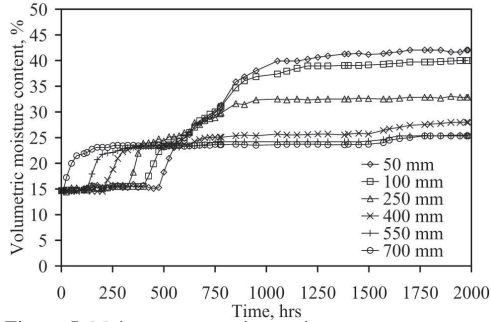infiltration rate was increased after 1500 hrs the moisture content at 700 mm increased to 25.4%.

Figure 5. Moisture content time series.

The data shown in Figure 5 may be further interpreted using isochrones of moisture content with height in the permeameter, shown in Figure 6. The data in this figure shows how the moisture content gradually progresses vertically downward through the profile. The accumulation of moisture at the base of the profile after 550 hrs is indicated by a bulge in the moisture profile at the base. The steady-state moisture content at the top of the profile is 23.5% after 1200 hrs for the first infiltration rate, and 25.3% after the second infiltration rate. During these two stages, it is clear that a unit hydraulic gradient is present in the upper portion of the soil profile (*i.e.*, the suction does not change with height). In this case the hydraulic conductivity is equal to the applied flow rate.

As mentioned, the suction values measured using the heat dissipation units was unreliable. Accordingly, the suction time series was predicted from the moisture content time series using the SWRC, as shown in Figure 7. The initial suction in the profile is approximately 166 kPa. After reaching steady-state infiltration, the suction in the upper portion of the specimen was about 20 kPa, while the suction at the base was approximately 1 kPa (near saturation).
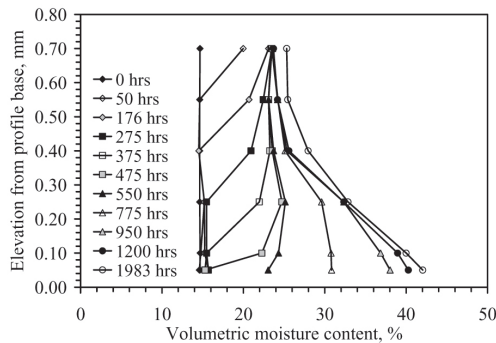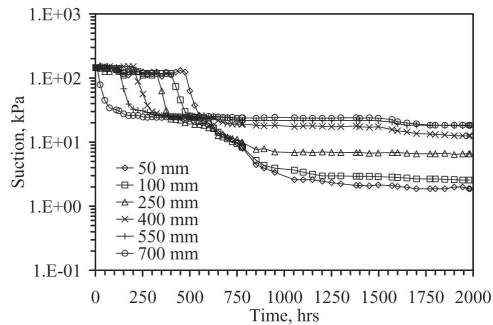

Figure 6. Moisture content profiles.

Figure 7. Suction values predicted from the WRC.

The raw θ and ψ data can be used to predict the K-function using Equation (3). The K-function values were calculated using measured data from the instantaneous profile method and from steady-state moisture profiles are shown in Figure 8. Data until 550 hrs was used in the instantaneous profile method. The van Genuchten-Mualem model K-function prediction is shown as well, although it cannot be strictly compared with the data from the instantaneous profile method because the WRC was used to calculate the suction values in the gradient term. The K-function data from the steady-state infiltration data is several orders of magnitude greater than the predicted K-function.

The instantaneous profile method data does not align perfectly with the steady-state data because the WRC used to calculate the suction values only fits the infiltration θ-ψ data at high suctions. At low suctions, the wetting-path WRC would have given more reliable calculations. The scatter arises from variability in the gradient term. Fluctuations in the suction have a large effect on the calculated K values as the gradient is in the denominator of Equation (3), and because the gradient contains the difference between two large numbers. Fluctuations in the measured moisture content time series were found to lead to negative or underestimated values of $\Delta V_{w,i}$. This led to low calculated K values.
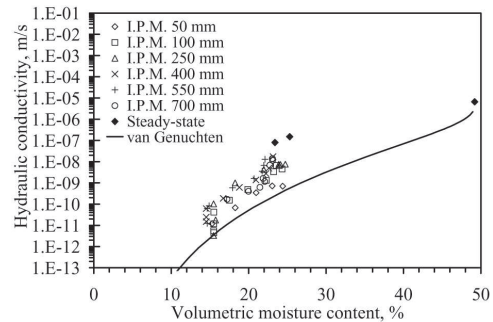

Figure 8. K-function calculated using measured data .

VI Simpósio Brasileiro de Solos Não Saturados 2007/ Salvador-Bahia

An approach to improve the instantaneous profile method calculations is to fit a smooth function to the moisture content and suction time series. The initial portion of the moisture content time series are the most useful for transient flow calculations, as there is a transition from dry soil to wet soil without the influence of the bottom boundary on the moisture profile. The initial portions of the curves follow an S-shaped curve, which is well represented by a sigmoid curve. The sigmoid curve used for matching the moisture content time series is:

$$\theta(t) = \frac{1}{a + be^{-ct}} \tag{10}$$

where t is time, e is the base of the natural logarithm, and a, b, and c are shape parameters. The shape parameter a may be calculated as:

$$a = \frac{1}{\left(\theta_{max} - \theta_{min}\right)} \tag{11}$$

where θ_{max} and θ_{min} are the maximum and minimum moisture contents in an S-shaped time series. If c is assumed to fit the curve, then b can be calculated as:

$$b = \frac{a}{t_\Delta c} \tag{12}$$

where t_Δ is the time at which the moisture content time series transitions from dry to wet. The sigmoid-fitted moisture content and suction time series calculated are shown in Figures 9(a) and 9(b).

These curves are only shown until 550 hrs, when the wetting front reaches the base of the profile. The fitted time series may be used to calculate the K-function with the instantaneous profile method, as shown in Figure 10. The K-function calculated using the fitted data and the instantaneous profile method shows slightly less scatter than the K-function shown in Figure 8. No negative K values were calculated. The transient and steady-state K functions do not match perfectly in this case either, because the drying-path WRC was used to calculate the suction values. A K-function that fits the steady-state data and the calculated K values at low moisture contents is also shown in Figure 10. This K-function does not follow the trend in the transient data for moisture contents greater than 18%. However, the steady-state moisture content values are certainly points on the K-function, so a fitted K-function should pass through these points.
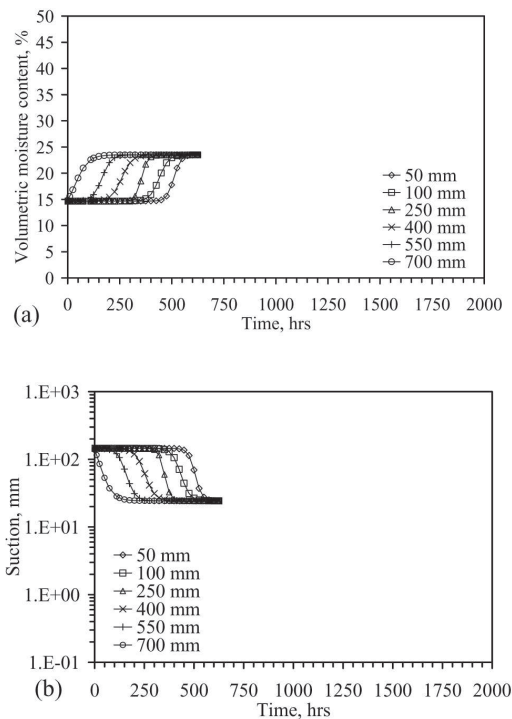

Figure 9. Moisture content time series fitted using the Sigmoid function for K-function analysis.
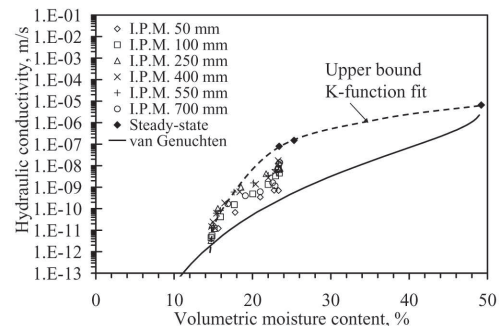

Figure 10. K-function calculated using sigmoid-fitted data.

4   CONCLUSIONS

Steady and transient infiltration data were used to compliment each other to define the K-function for low-plasticity clay over a wide range of volumetric moisture content values. The important issues involved with calculation of the K-function from

transient and steady-state infiltration were summarized in this study. These issues include outflow boundary effects on the moisture profile, the use of the water retention curve (WRC) to calculate suction values from measured volumetric moisture content values, calculation of the gradient terms, and fitting of the time series with smooth curves. The moisture profile was altered by the outflow boundary in the lower 500 mm of the profile. Only the measurements of moisture in the upper portion of the profile was used for the steady-state K-function calculation, and only the initial infiltration phase before the wetting front reached the base could be used for the transient analysis. The WRC should represent the relationship between θ and ψ throughout the infiltration process. The K function is particularly sensitive to fluctuations in the suction and moisture content, which can cause errors in the gradient and negative moisture storage values. Fitted sigmoid curves were found to represent the moisture content and time series well. The K-function predicted from the shape of the WRC was found to under-estimate the values of K.

5 REFERENCES

Childs, E. and Collis-George. N. (1950). The permeability of porous materials. Proc. Roy. Soc. London. A:201, 392-405.

Benson, C. and Gribb, M. (1997). Measuring unsaturated hydraulic conductivity in the laboratory and field. Unsaturated Soil in Engineering Practice. ASCE. 113-168.

Burdine, N. (1953). Relative permeability calculations from pore-size distribution data. Pet. Trans. Am. Inst. of Mining and Met. Eng. 198, 71-77.

Butters, G. and Duchateau, P. (2002). Cont. flow method for rapid measurement of soil hydraulic properties. VZJ. 1:239–251.

Conca, J., and Wright, J. (1992). Diffusion and flow in gravel, soil, and whole rock. *Applied Hydrogeology*. 1, 5-24.

Eching, S. and Hopmans, J. (1993). Optimization of hydraulic functions from transient outflow and soil water pressure data. SSSAJ. 57, 1167-1175.

Gardner, W. (1956). Calculation of capillary conductivity from pressure plate outflow data." SSSA Proc. 20, 317-320.

Gardner W. (1958). Some steady-state solutions of the unsaturated moisture flow equation with applications to evaporation from a water table. Soil Sci. 85, 228-232.

Meerdink, J., Benson, C., and Khire, M. (1996). Unsaturated hydraulic conductivity of two compacted barrier soils. ASCE JGGE. 122(7), 565-576.

Moore, R. (1939). Water conduction from shallow water tables. Hilg. 12, 383 426.

Mualem, Y. (1976) "A new model for predicting the hydraulic conductivity of unsaturated porous media. WRR 12,513-522.

Olson, R. and Daniel, D. (1981). Measurement of the Hydraulic Conductivity of Fine Grained Soils. ASTM STP 746, 18-64.

Parker, J., Kool, J., and van Genuchten, M. (1985). Determining soil hydraulic properties from one-step outflow experiments by parameter estimation: II Experimental studies. SSSAJ. 49,1354-1359.

Richards, L. (1952). Water conducting and retaining properties of soils in relation to irrigation. *Proc. Int. Symp. On Desert Res.*. 523-546.

Topp, G., Davis, J., and Annan, A. (1980). Electromagnetic determination of soil water content: Measurements in coaxial transmission lines. WRR. 16:574-582.

van Dam, J., Stricker, J., and Droogers, P. (1994). Inverse method to determine soil hydraulic functions from multi-step outflow experiments. SSSAJ. 58, 647-652.

van Genuchten, M. (1980). A closed-form equation for predicting the hydraulic conductivity of unsaturated soils. SSSAJ. 44, 892-898.

Wang, X. and Benson, C. (2004). Leak-free pressure plate extractor for the soil water characteristic curve. ASTM GTJ. 27(2),1-10.

Watson, K. (1966). "An instantaneous profile method for determining the hydraulic conductivity of unsaturated porous materials." WRR. 2(4), 709-715.

Wendroth, O., Ehlers, W., Hopmans, J., Kage, H., Halbertsma, J., and Wosten, J. (1993). "Reevaluation of the evaporation method for determining hydraulic functions in unsaturated soils." SSSAJ. 57, 1436-1443.

Wildenschild, D., Jensen, K., Hollenbeck, K., Illangasekare, T., Znidarcic, D., Sonnenborg, T., and Butts, M. (1997). A two stage procedure for determining unsaturated hydraulic characteristics using a syringe pump and outflow observations.